Buletinul Ştiinţific al Universităţii Politehnica Timişoara

TRANSACTIONS on ELECTRONICS and COMMUNICATIONS

Volume 60(74), Issue 1, 2015

Performance of Turbo Encoders with 64-QAM Modulators Interfacing Systems in Fading Environment

Maria Kovaci[1] Horia Balta[1,2]

Abstract – This paper presents a study on the interfacing between the turbo encoder and modulator. The binary allocation of the bits from a turbo coded symbol towards the modulator symbol can be done in several ways. This study shows the performance of the allocation modes taking into account the quadrature amplitude modulation with 64 points and the Rice fluctuating transmission channel. The simulations presented show that the performance of the entire transmission system, measured in coding gain may be influenced by up to 1 dB by a suitable choice of the allocation method.

Keywords: fading channel, communication systems, mapping, quadrature amplitude modulation, turbo code

I. INTRODUCTION

One of the most used modulations in the current communications systems is undoubtedly the Quadrature Amplitude Modulation (QAM). QAM is among the specifications of communications standards. Under its different variants, QAM is used in digital cable television or wireless and cellular technology applications. The 64-QAM is a good compromise between spectral efficiency (6 bit/s/Hz) and performance of bit/frame error rate (B/FER) versus signal to noise ratio (SNR) [1]. 64-QAM gives a symbol error rate of 10^{-6} for a SNR of about 19 dB for uncoded system in non-fluctuating channel (i.e., Additive White Gaussian Noise channel – AWGN channel) and, practically, it cannot be used in fading channel. However, using a turbo code, a BER of 10^{-10} can be obtained at a SNR of 9 dB for the AWGN channel and at SNR of 13 dB for the pure fluctuant channel (Rayleigh channel). Obviously, the advantages are the spectral efficiency and the simplicity of the implementation. For these reasons, the square 64-QAM is the most frequently digital modulation encountered in applications. For example, in LTE is specified that such modulation techniques with Gray allocation can be used to minimize the BER [2].

Of course, there are also disadvantages. One of them is that constellations with QAM modulations Gray allocation does not protect equally all the bits of the modulator symbol. Neither the 64-QAM modulation constellations is no exception to this. The problem arising is to find the binary allocation variant between the coded symbol and the modulator symbol which optimizes the performance. Our previous studies have been dedicated to this question for QAM constellations [3], [4], [5], in AWGN channel. In the present paper we study the turbo coded bit allocation for the 64-QAM constellations in Rice fading environment. A similar study, for 16-QAM was done in [6]. In this study we used both the double binary turbo code (DBTC) of the DVB-RCS2 standard [7] and the single binary turbo code (SBTC) of the LTE standard [2].

The Rice channel to which we referred above is a model for the real channels in which the received signal is a mixture between the direct wave (Line of Sight– LOS) which is propagated directly from the transmitter to the receiver and the waves reflected by different objects.

In this paper, as in [5], we have analysed three locations for the placement of the information and parity bits generated by turbo coding in the symbol modulator. In the first case the information bit was placed in the best protected position, followed by two parity bits placed in less protected positions. In the second case the information bit is placed on the middle position, so that in the better and less protected positions are placed the parity bits. Finally, in the third case, the information bit appears on the poorly protected position. The results of simulations show a completely different behaviour in the performance of B/FER vs SNR of these allocation variants.

The structure of this work is organized as follows. In Section II are presented the turbo encoders used in this paper (single binary - SBTE and double binary - DBTE) in order to identify the bits to be allocated in the symbol modulator. Section III briefly describes the square 64-QAM with the same aim to identify positions from the modulator symbol that will be filled by turbo encoded bits, nominated previously. Section IV is dedicated to presenting allocation alternatives. Section V shows the simulation results and Section VI concludes the paper.

[1] Faculty of Electronics and Telecommunications, Communications Dept.
Bd. V. Parvan 2, 300223 Timisoara, Romania, e-mail: maria.kovaci@upt.ro
[2] Valahia University of Targoviste, 2 Avenue King Carol I, 130024, Romania, e-mail: horia.balta@upt.ro

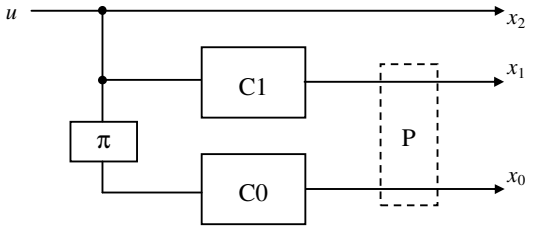

Fig. 1. The scheme of the SBTE.

II. THE TURBO ENCODER

The direct coupling between the turbo encoder and the modulator supposes the representation of the turbo coded block under a periodical structure form, with a period equal to the modulator symbol length. The structure of a turbo coded block is influenced by the structure of the turbo encoder and puncturing matrix. This section describes the SBTE specified in [2] and the DBTE specified in [7], configured for the coding rate 1/3 and 2/3, respectively.

A. *Single binary turbo encoder*

Fig. 1 shows the structure of a SBTE. Input sequence u is encoded directly by the convolutional encoder C1 and via interleaver (π) by the encoder C0. Depending on the requirements, the outputs of the two convolutional encoders are punctured to obtain higher coding rate. It follows redundant sequences x_0 and x_1, which, along with the original information sequence $u=x_2$ form SBTE's output. In the absence of puncturation, the (natural) encoding rate of SBTE's is 1/3. At this rate, the turbo coded block size is $3\times N_S$ where N_S is the length of interleaving. In other words, one turbo coded block consists of N_S symbols of the form $x_j=(x_2^j, x_1^j, x_0^j)$, with j from 0 to N_S-1.

B. *Double binary turbo encoder*

Fig. 2 shows the scheme of a DBTE. Unlike SBTE, a DBTE generates a four-bit symbols $x_j=(x_3^j, x_2^j, x_1^j, x_0^j)$ at its natural rate 1/2. In this case the size of a turbo coded block is $4\times N_D$ where N_D is the length of inter-symbol interleaving. Note that DBTE performs both the inter-symbol interleaving (information symbols are interleaved) and the intra-symbol interleaving (the bits from information symbol are interleaved).

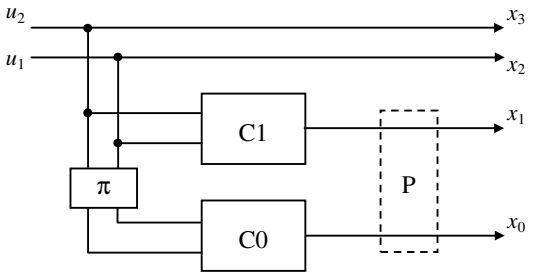

Fig. 2. The scheme of the DBTE.

Because the modulator symbol for 64-QAM contains 6 bits, three for each carrier, for compatibility, we chose to use the coding rate 2/3.
To obtain the coding rate 2/3 for DBTE. we have used the punctured matrix:

$$M_{pd}=\begin{bmatrix}1 & 0\\ 0 & 1\end{bmatrix}, \qquad (1)$$

which also applies to sequences x_1 and x_0. The structure of a turbo coded block is of the form:

$$\begin{aligned}&\ldots\ x_3^j,\ x_3^{j+1},\ \ldots\\ &\ldots\ x_2^j,\ x_2^{j+1},\ \ldots\\ &\ldots\ x_1^j,\qquad\ ,\ \ldots\\ &\ldots\qquad ,\ x_0^{j+1},\ \ldots\end{aligned}$$

with j from 0 to $(N_D/2)-1$.
Thus, in both cases (SBTE with coding rate 1/3 and DBTE with coding rate 2/3) we have obtained a periodic structure of the data block of 3 or 2×3 bits. These triplets of bits will form the modulator symbol for 64-QAM, symbol of 6 bits, as shown in the next section.

III. THE SQUARED 64-QAM

The constellations for 64-QAM square modulation is presented in Fig. 3. A signal modulated using squared 64-QAM has the form:

$$s_j(t)=p_j\cdot\varphi_1(t)+q_j\cdot\varphi_2(t),\quad j\in\{1,2,\ldots,64\}, \qquad (2)$$

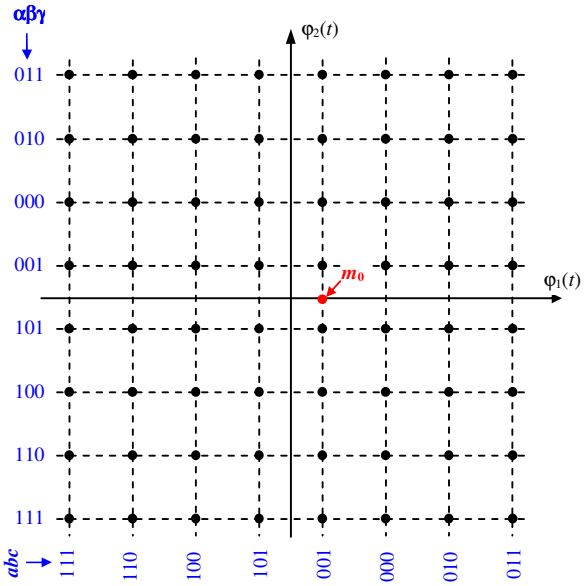

Fig. 3. Signal points constellation for square 64-QAM with Gray allocation.

where $\varphi_1(t)$ and $\varphi_2(t)$ are the in-phase and quadrature carriers, of unitary energy (1J). The coefficients p_j and q_j take values in the set $\{-7, -5, -3, -1, 1, 3, 5, 7\}\cdot m_0$, each of them depending by the 3 bits of the 6 bits of the modulating symbol, m_j, where:

$$m_j = [a_j\ \alpha_j\ b_j\ \beta_j\ c_j\ \gamma_j], \quad j \in \{1,2, \ldots ,64\}, \tag{3}$$

with α_j, β_j, γ_j, a_j, b_j, $c_j \in \{0,1\}$, and $m_0 = 1/\sqrt{42}$. (The bits order of m_j, (relation 3) and the m_0 value were chosen as in [2].) For a Gray allocation we have:

$$\begin{aligned} p_j &= (1-2\cdot a_j)\cdot(4+(2\cdot b_j-1)\cdot(2+(2\cdot c_j-1)))\cdot m_0 \\ q_j &= (1-2\cdot \alpha_j)\cdot(4+(2\cdot \beta_j-1)\cdot(2+(2\cdot \gamma_j-1)))\cdot m_0 \end{aligned} \tag{4}$$

The binary values for α_j and a_j determine the sign of the coefficients p_j and q_j (in negative logic) while the pairs (β_j, γ_j) and (b_j, c_j) determine their module. The bits β_j and b_j, are playing the role of the most significant bit, and γ_j and c_j are playing the role of the least significant bit. Thus, the 64-QAM square modulation will protect differently the bits of m_j. The most protected bits will be the sign bits, α_j and a_j, then bits from the pairs (β_j, b_j) and (γ_j, c_j).
The modulated signal is sent through a Rice flat fading channel. At the output of the demodulator it results a samples sequence with the form:

$$y_i = \alpha_i \cdot h_i + n_i, \tag{5}$$

where α_i is the amplitude of the Ricean fading, h_i is given by p_j or q_j, and n_i is a sample of the AWGN noise. The fading amplitude has a Rice probability distribution. A random variable with Rice distribution $\alpha = \sqrt{X^2 + Y^2}$ can be modeled as a sum of two normally distributed variables, with the same variance σ^2, one with zero mean, Y, and one with non-zero mean (A), X. The random variable X can be thought as:

$$X = Z + A, \tag{6}$$

where Z represents the normal random variable with zero mean and variance σ^2.
Thus, the random variable with Rice distribution, α, can be written as in:

$$\alpha = \sqrt{(Z+A)^2 + Y^2} = \sqrt{r^2 + 2\cdot A\cdot r\cdot\cos\Phi + A^2}\ , \tag{7}$$

where $r = \sqrt{Y^2 + Z^2}$ is a random variable with Rayleigh distribution; Φ is the phase of complex distribution whose real and imaginary parts are given by the random variables Y and Z.
The ratio of power of LOS component to the power of multipath component is called Ricean K factor, [8], defined as:

$$K = A^2 / (2\cdot\sigma^2), \tag{8}$$

In our simulations we assumed the total power $\alpha^2 = A^2 + r^2 = A^2 + 2\cdot\sigma^2$ to be unitary so $A^2 \in [0, 1]$.

IV. INTERFACING TURBO ENCODER AND 64-QAM MODULATOR

This section describes interconnection ways (interfacing) between the turbo encoder and modulator. For each turbo code and coding rate we have chosen three bits allocation ways, indicated by acronyms $q0$, $q1$ and $q2$, respectively. On the complete labeling of variants we have noted the SBTC with s, the DBTC with d and the encoding rates 1/3 and 2/3 with 33 or 67, respectively.

A. *CMBM variants for SBTC*

Variants of coding to modulation bit mapping (CMBM) for SBTC with coding rate 1/3 are shown in Table 1. Since the natural coding rate of SBTC is 1/3, in this case the bits allocation for in-phase component is identical to those of the quadrature component. What is different is only the position of the modulator symbol m_j in which the information bit x_2 will be placed. In the first case $s33q0$, x_2 is the most protected bit (with role of a_j or α_j). In the second case $s33q1$, x_2 is the middle bit (with role of b_j or β_j) and in $s33q2$ case, x_2 is the least protected bit (with role of c_j or γ_j).

B. *CMBM variants for DBTC*

We used 2/3 coding rate for DBTC. CMBM variants in this case are shown in Table 2. Because of the symmetry, we chose the symbol bits (generated by DBTE) with even index to be assigned to in-phase component and the symbol bits with odd index to be assigned to odd symbols. By doing so, we will have 2 information bits and only one parity bit for triplets (a_j b_j c_j) and (α_j β_j γ_j). The cases chosen and presented in Table 2 differ by positioning the parity bit.

Table 1
CMBM Variants for SBTC and a Coding Rate of 1/3

	a_j, α_j	b_j, β_j	c_j, γ_j	**protects**
$s33q0$	x_2	x_1	x_0	information
$s33q1$	x_1	x_2	x_0	hybrid
$s33q2$	x_1	x_0	x_2	parity

Table 2
CMBM Variants for DBTC and a Coding Rate of 2/3

	in-phase			**quadrature**		
	a_j	b_j	c_j	α_j	β_j	γ_j
$d67q0$	x_3^j	x_2^j	x_1^j	x_3^{j+1}	x_2^{j+1}	x_0^{j+1}
$d67q1$	x_3^j	x_1^j	x_2^j	x_3^{j+1}	x_0^{j+1}	x_2^{j+1}
$d67q2$	x_1^j	x_3^j	x_2^j	x_0^{j+1}	x_3^{j+1}	x_2^{j+1}

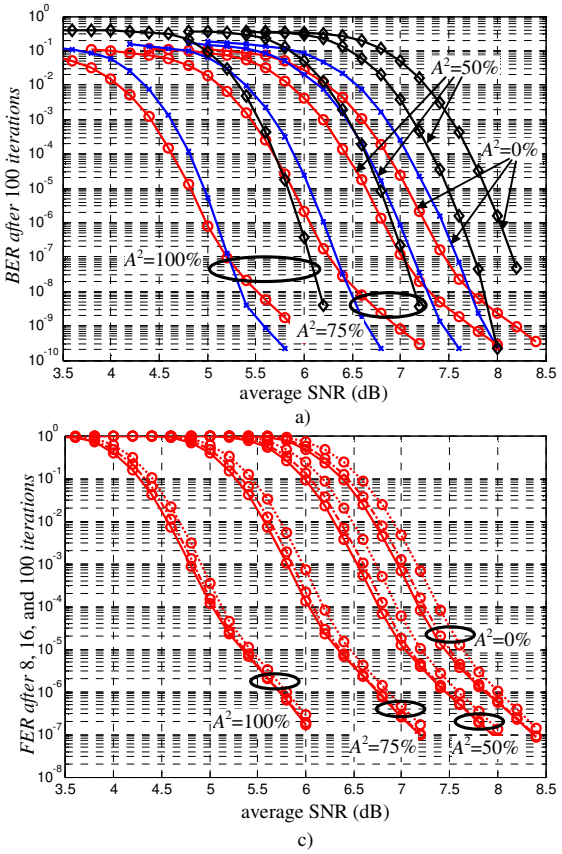

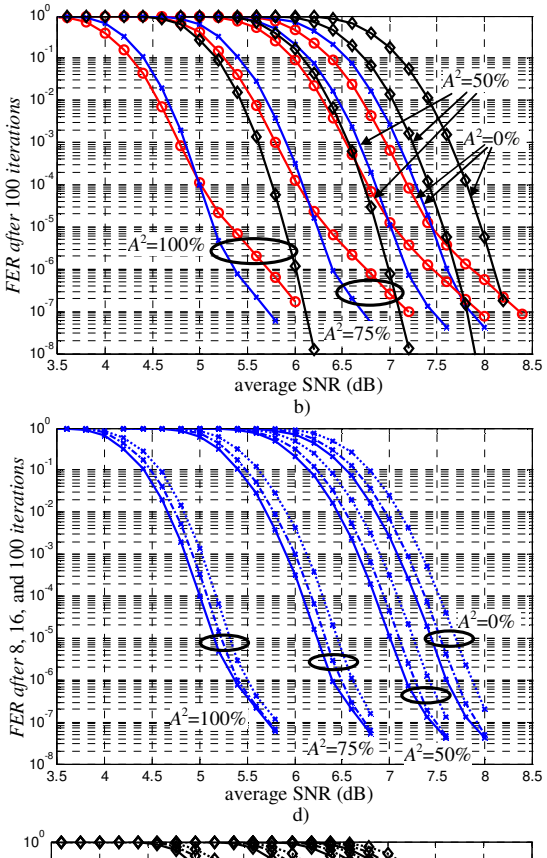

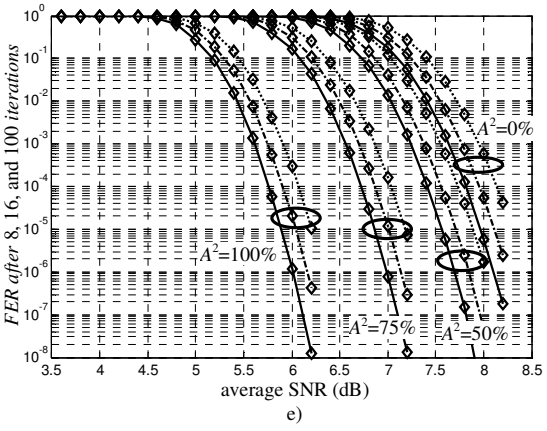

Fig. 4. The performances of memory 4 SBTC from [2] with the coding rate R_c = 1/3 and CMBM modes for 64-QAM: *s*33*q*0 – red-circles, *s*33*q*1 – blue-x, *s*33*q*2 – black-diamonds; with continuous line after 100 iterations, with dashed line after 16 iterations and with dotted line after 8 iterations.

V. EXPERIMENTAL RESULTS

This section presents the results of our investigations. More specifically, there are presented the performance of SBTC of LTE standard [2] and the performance of DBTC of DVB-RCS2 standard [7] using squared 64-QAM and all variants of CMBM presented in the previous section (Table 1 and 2).

A. *Turbo coding parameters used in the simulations*

In the simulations we considered the parameters of TCs specified in the two standards. We refer to the component convolutional encoders and to the specified interleaving methods. We have used the 1504 data bit blocks in all cases. For this reason we set N_S=2·N_D=1504. The circular closing method (tail biting) of the trellis was considered in all cases, [9].

We used the Max-Log-MAP algorithm for decoding [10], with a weighting of extrinsic information [11]. Extrinsic information weighting coefficients were 0.7 for SBTC and 0.75 in the DBTC case. We used also the genie iterations stopping criterion [12], with values for the maximum number of iterations of 8, 16 and 100. We considered a Rice channel with a percentage of the non-fluctuating wave power (LOS) with the values: 0% (Rayleigh channel), 50%, 75% and 100% (AWGN channel).

B. *Simulation results*

The simulation results are shown in Fig. 4 and Fig. 5. For each point of the curves shown in the diagrams of these figures, we have carried out simulations to

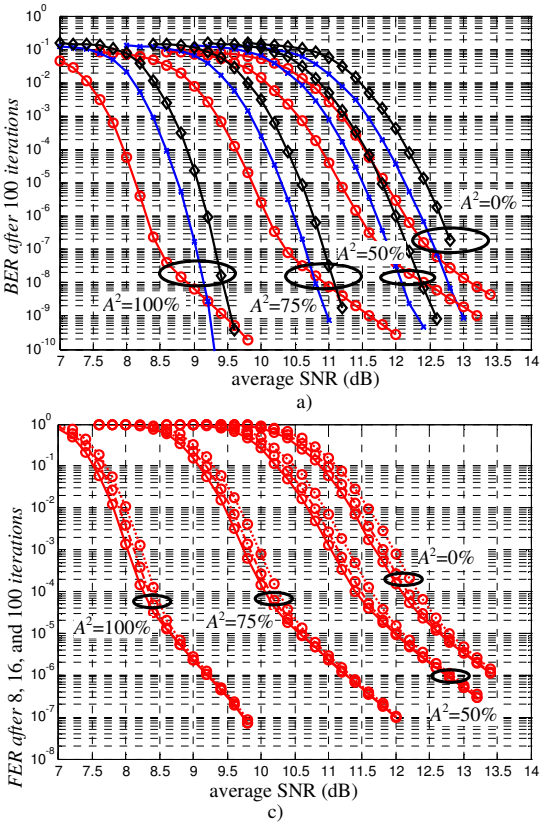

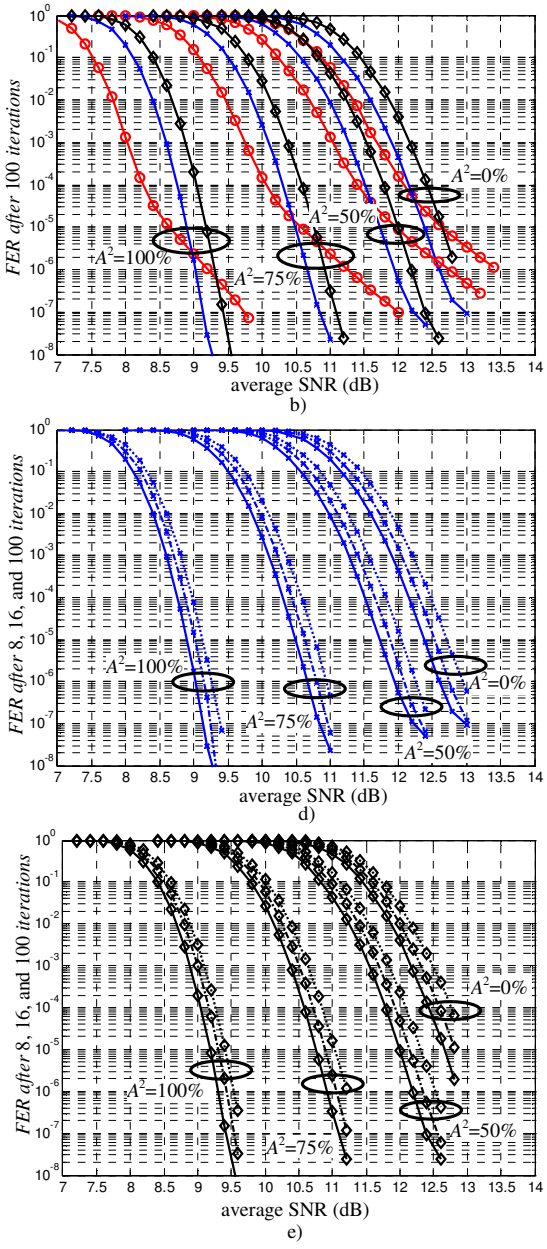

Fig. 5. The performances of memory 4 DBTC from [7] with the coding rate R_c = 2/3 and CMBM modes for 64-QAM: $d67q0$ – red-circles, $d67q1$ – blue-x, $d67q2$ – black-diamonds; with continuous line after 100 iterations, with dashed line after 16 iterations and with dotted line after 8 iterations.

obtain 500 erroneous blocks or to process a number of 10^9 data blocks.

Fig. 4 shows the performance of SBTC for each of the 3 CMBM variants given in Table 1, at a natural coding rate of 1/3. In the waterfall region, the curves built for the same value of A^2 (the percentage power of the non-fluctuating wave) are spaced with about 1 dB on SNR. The hierarchy on performance in this region is $s33q0$, $s33q1$ and $s33q2$, respectively. With the transition to error floor region of curves, the hierarchy changes, version $s33q0$ showing a more pronounced error floor effect. It is noticeable the consistent effect of the fluctuating component on performance. Thus, if only 25% of the total power is reflected in the fluctuating component, the system performance, in terms of coding gain, decreases at half (the curves denoted A^2= 75% are placed at mid-distance between the curves for A^2 = 100% – non-fluctuating channel and the curves for A^2 = 0% – pure fluctuating channel).

The curves in Fig. 5 show the performance of DBTC, with rate 2/3, for each of CMBM methods described in Table 2. Like the first case, here we have a large "spreading" of the curves in the waterfall region. Like in previous cases hierarchies are, in order of performance $d67q0$, $d67q1$, $d67q2$ for waterfall region and $d67q2$, $d67q1$, $d67q0$ for error floor region.

Also, as for SBTC, the curves obtained in this case for different values of the Ricean factor (the balance between the fluctuating component and non-fluctuating component) appear as some "echoes at right" of the AWGN channel curves.

Regarding the influence of the maximum number of iterations in turbo decoding on performance, we note a gain of about 0.1 dB in the waterfall region, from 8 to 16 iterations and from 16 to 100 iterations. This gain is canceled for curves in red-circles ($s33q0$ and

*d*67*q*0) in the error floor region, and tends to increase for the black-diamonds curves (*s*33*q*2 and *d*67*q*2). The phenomena are similar also for SBTC.

VI. CONCLUSIONS

First, we note that the relative performance of the different CMBM variants is practically independent of the value of A^2. Noteworthy is the big gap between the performance variants with information protection (...*q*0) and those with parity protection (...*q*2). This gap can reach the value 1 dB.

The variants "... *q*0" are the best in the waterfall region. They are followed, as performance, by the hybrid variants noted with "... *q*1". The worst performance in the waterfall region is obtained by the variants "…q2", in which the QAM modulation protection is on the parity bits. But, while the FER lowers, the curves obtained for the variants ".... q0". lose their superiority one after another in favour of other variants. In the bottom of the curves (the error floor region) appears a major difference in the gains brought by the performing of some additional iterations. Thus, if for variants "... *q*0" performing additional iterations is unnecessary for the other variants, the additional iterations bring a consistent coding gain. The explanation is the fact that at hybrid variant and at parity protection variant, the error floor region practically was not reached until the investigated FER values.

The hybrid variants (*s*33*q*1 and *d*67*q*1) which protect alternative the information bits and the parity bits are a good solution for the balance between the waterfall and the error floor regions. In SBTC the difference between the hybrid variant and the information bits protect variant is very small, so that the exchange in the hierarchy of performance between the two variants occurs earlier.

Therefore, the study presented in this paper recommends the CMBM hybrid variants.

ACKNOWLEDGEMENTS

This work was partially supported by the strategic grant POSDRU/159/1.5/S/137070 (2014) of the Ministry of National Education, Romania, co-financed by the European Social Fund – Investing in People, within the Sectoral Operational Programme Human Resources Development 2007-2013 and by a grant of the Romanian Ministry of Education, CNCS – UEFISCDI, project number PN-II-RUPD-2012-3-0122.

REFERENCES

[1] J.G. Proakis, *Digital Communications*, McGraw-Hill, 4th edition, 2001.

[2] ETSI, 3GPP TS 36.212: "Evolved Universal Terrestrial Radio Access (E-UTRA), Multiplexing and channel coding". http://www.etsi.org/deliver/etsi_ts/136200_136299/136212/08.08.00_60/ts_136212v080800p.pdf

[3] H. Balta, F. Alexa, and A. Vesa, "On the allocation of double-binary turbo coded bits in the case of 16-QAM modulation", Proceedings of the 11th International Symposium on Electronics and Telecommunications, ISBN 978-1-4799-7265-4, November 14-15, Timişoara, România, pp. 191-196, 2014.

[4] H. Balta, J. Gal, and C. Stolojescu-Crişan, "On the Double-Binary Turbo Coded Bits Allocation Mode in the Case of 256-QAM Square Modulation", Proceedings of the 37th International Conference on Telecommunications and Signal Processing (TSP), ISBN 978-80-214-4983-1, ISSN 1805-5435, July 1-3, Berlin, Germany, pp. 129-134, 2014.

[5] R. Lucaciu, M. Kovaci, J. Gal, A. Mihaescu, and H. Balta, On the Turbo Coded Bits Allocation Mode for the 64-QAM Square Modulation, 38th International Conference on Telecommunications and Signal Processing (TSP), July 9-11, Prague, Czech Republic, 2015.

[6] M. Kovaci, and H. Balta, A study on turbo coded 16-QAM bit allocation in Rice flat fading channel, The 10th International Conference on Future Networks and Communications (FCN 2015), August 17-20, Belfort, France, 2015.

[7] European Telecommunications Standards Institute, "DVB Interactive Satellite System, Part 2: Lower Layers for Satellite standard", DVB Document A155-2, March 2011. Available: http://www.dvb.org /technology/standards/a155-2_DVB-RCS2_Lower_Layers.pdf.

[8] F. Vatta, G. Montorsi, F. Babich, "Analysis and Simulation of Turbo Codes Performance over Rice Fading Channels", IEEE International Conference on Communications, ICC 2002, 28 April-2 May, 2002, New York City, NY, USA, vol.3, pp. 1506-1510.

[9] C. Weiss, C. Bettstetter, S. Riedel, and D. J. Costello, "Turbo decoding with tailbiting trellises", in *Proc. IEEE Int. Symp. Signals, Syst., Electron.*,Pisa, Italy, pp. 343–348, Oct. 1998.

[10] W. Koch, and A. Baier, "Optimum and sub-optimum detection of coded data disturbed by time-varying intersymbol interference." *In Proc. GLOBECOM* '90, pp. 1679-1684, December 1990.

[11] H. Balta, and C. Douillard, "On the Influence of the Extrinsic Information Scaling Coefficient on the Performance of Single and Double Binary Turbo Codes", Advances in Electrical and Computer Engineering, Vol. 13, No. 2, pp. 77-84, May 2013.

[12] A. Matache, S. Dolinar, and F. Pollara, "Stopping Rules for Turbo Decoders", *TMO Progress Report 42-142*, August 2000, Jet Propulsion Laboratory, Pasadena, California.